

# EPITAXIAL SILICON MICROSHELL VACUUM-ENCAPSULATED CMOS-COMPATIBLE 200 MHz BULK-MODE RESONATOR

Kuan-Lin Chen<sup>1</sup>, Hengky Chandrahilim<sup>2</sup>, Andrew B. Graham<sup>1</sup>,  
Sunil A. Bhawe<sup>2</sup>, Roger T. Howe<sup>1</sup> and Thomas W. Kenny<sup>1</sup>

<sup>1</sup>Stanford University, Stanford, California, USA

<sup>2</sup>Cornell University, Ithaca, New York, USA

## ABSTRACT

This paper shows the first successful combination of dielectrically-transduced 200 MHz resonators with the epi-silicon encapsulation process, and demonstrates a set of important capabilities needed for the construction of CMOS-compatible RF MEMS components. The result shows the resonant frequency of 207 MHz and a quality factor of 6,400. The high  $fQ$  ( $1.2 \times 10^{12}$  Hz) makes this encapsulated resonator an excellent candidate for applications in local oscillators and RF spectrum analyzers.

## INTRODUCTION

Wireless communication has greatly impacted our daily lives since the first radio system was invented [1]. Applications, such as cellular phones, satellite television, GPS navigation, and wireless internet networks, are driving the development of RF components in the direction of being smaller, more inexpensive and requiring less power, and thus this topic has been one of the hottest research areas. MEMS resonators have great potential for replacing conventional resonators used in portable wireless applications because of their merits of small size, high quality factor ( $Q$ ), and low power consumption [2]. There is also great interest in using coupled micro-resonators as band-pass filters and several research groups have already demonstrated exciting results [3-4].

Despite the advances in device performance, packaging for MEMS resonators remains a critical challenge. Because of their extreme sensitivity to the environment, MEMS resonators need vacuum encapsulation to achieve high quality factors ( $Q$ ) and enable post-MEMS CMOS integration. The promising on-chip application also requires a CMOS compatible packaging process. Due to the stringent RF requirements, the electrical properties and hermeticity of the packaging are also very important.

This paper presents the design, fabrication, packaging design, and measurement of a 200 MHz, dielectrically-transduced, width-extensional mode resonator encapsulated in an epitaxial-grown silicon package. The paper also explains the challenges of merging two technologies into a promising solution of a high frequency MEMS-based device.

## DESIGN OF RESONATOR

Dielectrically-transduced silicon bar resonators vibrating in the bulk-mode have superior linearity and high quality factors [5, 6]. The width-extensional mode resonance of a bar resonator depends on the width,  $W$ , with frequency

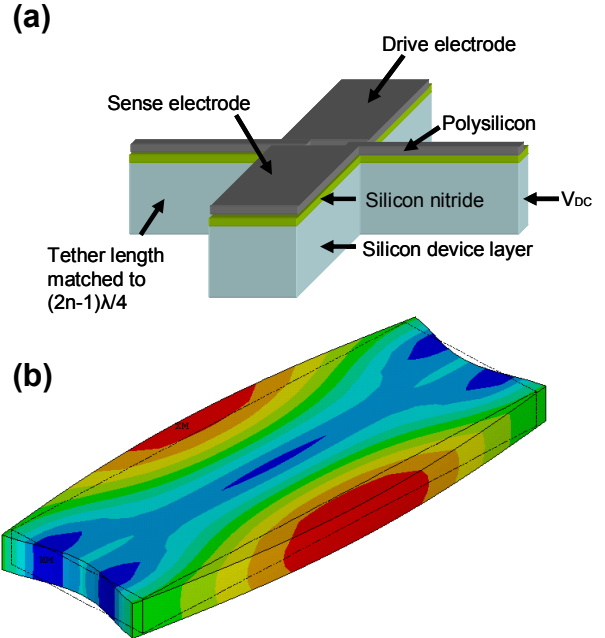


Figure 1: (a) Schematic diagram of the dielectrically-transduced, width-extensional mode resonator and (b) ANSYS contour plot of the width-extensional bar mode shape.

$$f = \frac{n}{2W} \sqrt{\frac{E}{\rho}}$$

where  $n$  is the mode number ( $n = 1, 3, \dots$ ), and  $E$  and  $\rho$  are the effective elastic modulus for 2D expansion and the density of silicon, respectively. The width-extensional mode is excited by patterning electrodes in plate configuration on top of the resonator using dielectric transduction, as shown in Fig. 1(a). The main bar resonator consists of three layers - a 100nm polysilicon electrode layer, a 100nm silicon nitride transducer layer, and a  $3\mu\text{m}$  single-crystal silicon resonator layer. As shown in Figure 1, the input and output electrodes are patterned on polysilicon and the silicon nitride layer is used as a high- $\kappa$  dielectric to enhance the transduction (compared to an air-gap). The quarter-wavelength anchoring scheme is designed to minimize mass-loading of the resonator. A DC bias is superimposed on a small AC voltage using a Bias-T and applied to the drive electrode, while the silicon device layer is connected to RF ground. This time-varying voltage causes a squeezing force on the dielectric thin film. Due to the Poisson effect, the dielectric layer experiences a lateral strain. Since the silicon nitride layer is structurally integrated with the silicon bar, the lateral strain is transferred from the dielectric film to the silicon resonator layer. As the strain distributes through the resonator, the width-extensional

mode is excited and the motional current is sensed through the sense electrode. The ANSYS fundamental mode shape of the width-extensional resonator is shown in Fig. 1(b).

## EPITAXY-SILICON PACKAGING (MICROSHELL)

The fabrication process is the fusion of two technologies developed at Cornell and Stanford [6, 7]. The wafer-level encapsulation packaging developed at Stanford University has the advantage of a small foot print, superior long-term stability, and CMOS compatibility [8-10]. The epitaxial-grown silicon allows CMOS circuitry to be built on top of the package to be integrated with the MEMS device packaged inside.

Previously, there have been accelerometers and resonators working at 1.2–1.4 MHz or below, encapsulated in this packaging. However, there has not been an attempt to encapsulate devices with resonant frequencies higher than 20 MHz using this silicon package. A thorough study of the electrical performance of the packaging was investigated [11]. The paper indicates that the silicon vertical interconnect has less than 1 dB attenuation up to 6 GHz, which extends the utility of this packaging for IF to HF resonator applications.

## FABRICATION

As shown in Fig. 2, the fabrication begins with a silicon-on-insulator (SOI) wafer with a device layer of 3 $\mu\text{m}$ . A stack of 100nm stoichiometric silicon nitride and 100nm heavily doped n+ polysilicon was deposited using low pressure chemical vapor deposition (LPCVD). The polysilicon layer was patterned to create electrodes. Part of the silicon nitride layer was etched to create electrical contact to the device layer, as shown in Fig. 2(b). The resonator was then patterned and etched through the nitride/silicon stack using deep reactive ion etching (DRIE). Low temperature oxide (LTO) was deposited as the sacrificial layer to create a cavity on top of the resonator. The LTO was then patterned and etched to create electrical contacts.

The main challenge is in creating low-loss vertical interconnects making contact to two different layers of the resonator. As shown in Fig. 2(d), the LTO was patterned and etched to create an electrical connection to the polysilicon layer as well as the device layer. Due to the thickness variation from the LTO deposition, stopping the etch on two different layers is extremely challenging using an academic-grade plasma etcher (insufficient etching selectivity, non-uniform etching across the wafer, etc.) However, this challenge can be greatly reduced with an industry-grade etcher.

Another challenging issue is the resistivity of the epi-polysilicon interconnects. A lot of characterization was done to ensure the resistivity of the epi-polysilicon was less than 10 m $\Omega\text{-cm}$ . Highly phosphorus doped epi-silicon was then grown on the top of the wafer to encapsulate the resonators. Vent holes were patterned to open access to the sacrificial LTO. A custom made HF vapor etcher in the Stanford Nanofabrication Facility was used to release the resonator. After releasing, vent holes were again sealed by LTO in a low pressure environment to vacuum-

encapsulate the resonators. Finally, an aluminum layer was used for electrical interconnects and bond pads. An SEM picture of a fabricated width-extensional mode resonator is shown in Fig. 3.

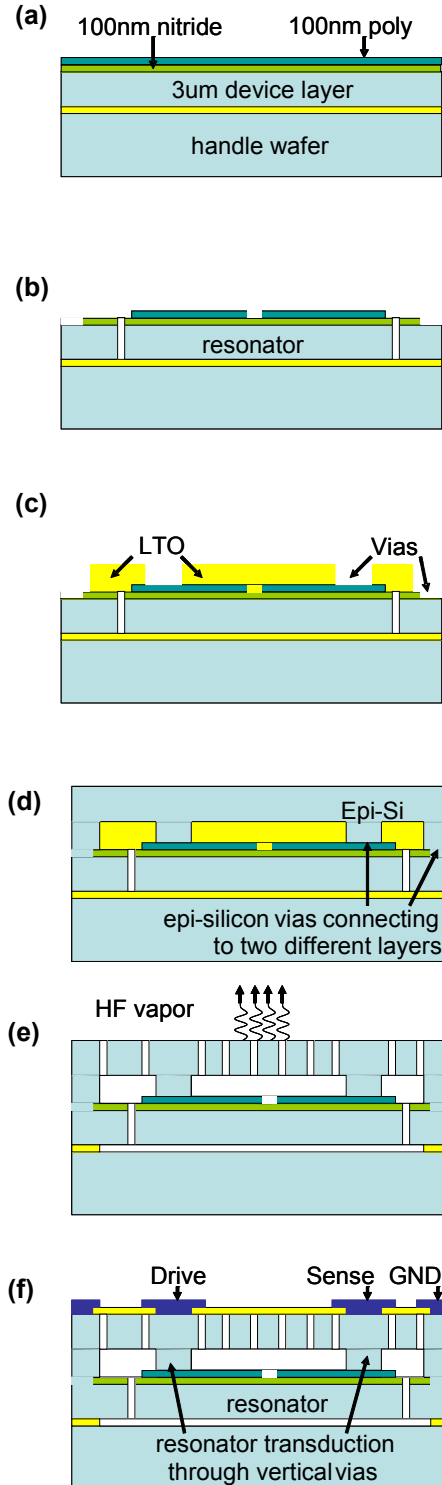


Figure 2: Epi-silicon microshell encapsulation process for dielectrically transduced resonators. Vertical epi-vias to the poly electrodes provide RF input/output while the vias to the silicon device layer provide a micro RF-cage providing a shielded microenvironment.

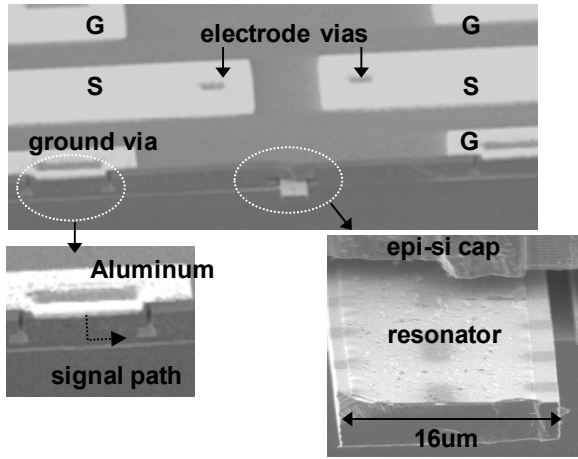


Figure 3: SEM of the fabricated resonator. The zoomed-in picture on the right shows the thin poly electrode on top of the resonator bar. The zoomed-in picture on the left shows the electrical contact between the epi-silicon and the device layer.

## DIFFERENTIAL MEASUREMENT SETUP

As shown in Fig. 4, a simple two-port measurement gives a clear sharp dip in  $S_{21}$ , indicating the electromechanical resonance is masked by the parasitic feedthrough. To overcome the capacitive feedthrough, the resonator was characterized using a differential measurement technique, inspired by [12, 13]. An RF signal from the network analyzer first goes into a splitter to create in-phase and out-of-phase signals, represented by  $+RF_{in}$  and  $-RF_{in}$ , respectively. In order to induce resonance of the resonator, a DC bias,  $V_{DC}$ , was added into  $+RF_{in}$  using a Bias-T. Two identical resonators were driven by  $+RF_{in}$  and  $-RF_{in}$ . While  $+RF_{in} + V_{DC}$  was driving the resonator, the pure AC  $-RF_{in}$  was driving the dummy resonator, with only its parasitic capacitance being driven. The outputs from both structures were then mixed together, where the out-of-phase current from the parasitic capacitance cancels out the parasitic component in the signal from the resonator. The exact differential

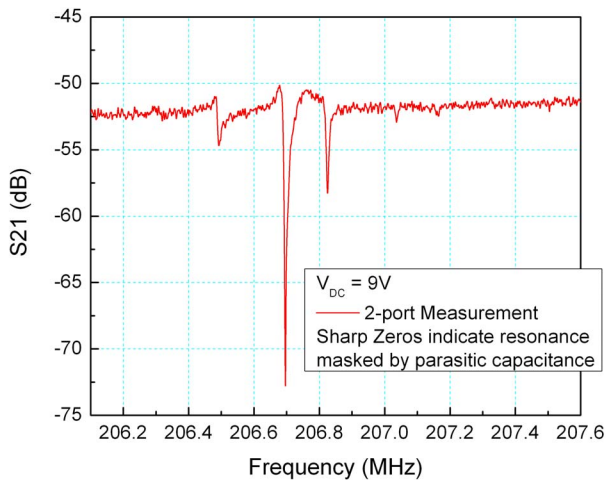


Figure 4: Transmission response using the 2-port measurement. Capacitive feedthrough masks the electromechanical resonance, resulting in a sharp dip at the target frequency.

measurement setup used in this work is express in Fig. 5. Although it would be ideal to have two identical resonators side-by-side when the differential measurement is conducted, the fabricated wafer only has a similar resonator by its side. Therefore, although the improvement of the signal to noise ratio is already greatly enhanced by using a similar structure as the dummy resonator, the feedthrough cancellation is not yet optimized.

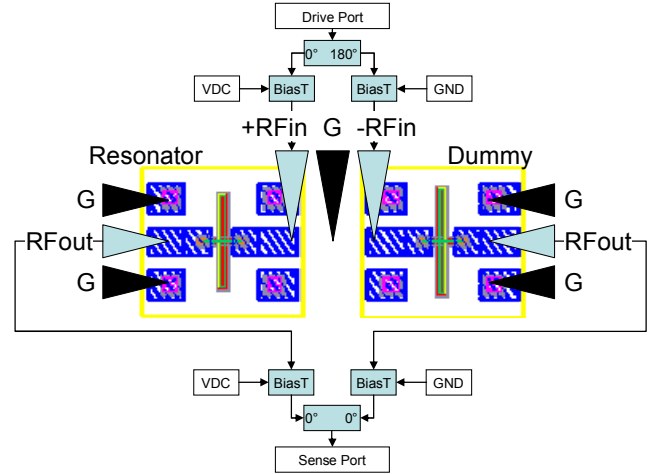


Figure 5: Schematic of the pseudo-differential measurement setup.

## RESULT

From the SEM picture, one can observe that the vertical interconnect is firmly connected to the device layer, providing electrical ground to the resonator beam. One can also note that the thin ( $\sim 13\mu\text{m}$ ) epi-silicon is enough to provide mechanical stability for the low-pressure hermetic packaging. It is important to keep this layer thin because of the electrical requirements [11].

The fabricated resonator was measured using the differential measurement setup explained in the previous section. Fig. 6 shows the response using feedthrough cancellation on top of the response from the 2-port

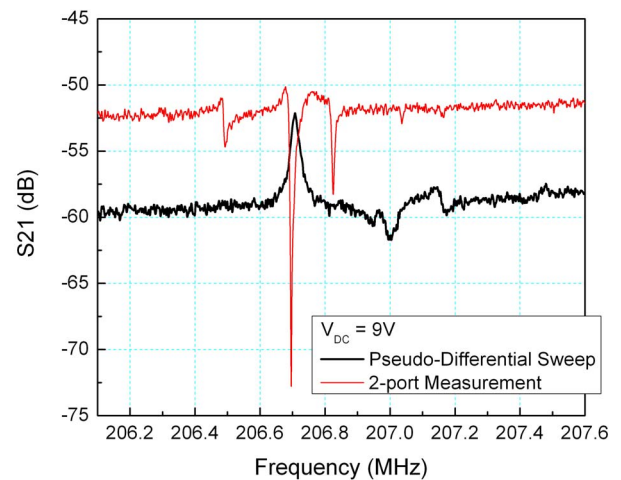


Figure 6: Transmission responses of the simple 2-port measurement and pseudo-differential measurement. It is clearly shown that the resonance peak matches the sharp dip shown in the 2-port measurement.

measurement. The resonant frequency is 207 MHz and the quality factor is 6,400. This is the highest reported frequency for a MEMS resonator packaged in a microshell. One can also note that there is a -13 dB noise reduction due to the implementation of the differential measurement.

## CONCLUSION

A fully encapsulated, width-extensional mode resonator was successfully fabricated with an  $fQ$  product of  $12 \times 10^{11}$  Hz, making it an excellent candidate for drop-in insertion in local oscillator and RF spectrum analyzer applications. The performance of the epitaxial-silicon packaging is also verified to sufficiently package VHF devices.

In the future, we plan to introduce Hafnium dioxide ( $\text{HfO}_2$ ) as the dielectric film to reduce the motional impedance. Furthermore, the length of the width-extensional mode resonator can be increased to enlarge the transduction area. Hence, the motional impedance of the encapsulated resonator could be reduced and alleviate the challenge of impedance matching.

## ACKNOWLEDGEMENTS

The authors would like to thank the staff in the Stanford Nanofabrication Facility, Gary Yama from Robert Bosch LLC RTC, and other people who work in the SNF for technical support.

This work was supported by a subaward on the DARPA Analog Spectral Processors program, with Chris Conway of Rockwell Collins as PI. The authors gratefully acknowledge the financial support from the DARPA Analog Spectral Processors program for this project (contract #N00173-06-C-2055). Distribution Statement "A" (Approved for Public Release, Distribution Unlimited).

## REFERENCES

- [1] G. Marconi, "Wireless telegraphy," Smithsonian Institution, Washington, D.C., Annual Report – 1901, 1902, pp. 287-298.
- [2] Y.-W. Lin, S. Lee, S.-S. Li, Y. Xie, Z. Ren, and C. T.-C. Nguyen, "60-MHz wine glass micromechanical disk reference oscillator," Digest of Technical Papers, 2004 IEEE International Solid-State Circuits Conference, San Francisco, California, Feb. 15-19, 2004, pp. 322-323.
- [3] S.-S. Li, Y.-W. Lin, Z. Ren, and C. T.-C. Nguyen, "A micromechanical parallel-class disk-array filter," Proceedings, 2006 IEEE Int. Frequency Control Symp., Geneva, Switzerland, May 29-June 1, 2007, pp. 1356-1361
- [4] G.K. Ho, R. Abdolvand, and F. Ayazi, "Through-Support-Coupled Micromechanical Filter Array," Proc. IEEE Micro Electro Mechanical Systems Conference (MEMS '04), Maastricht, the Netherlands, Jan. 2004, pp.769-772.
- [5] Hengky Chandralalim and Sunil A. Bhave, "Digitally-tunable MEMS filter using mechanically-coupled resonator array," 21<sup>st</sup> IEEE International Conference on Micro Electro Mechanical Systems (MEMS 2008), Tucson, Arizona, January 13-17, 2008, pp. 1020-1023.
- [6] Sunil A. Bhave and Roger T. Howe, "Silicon nitride-on-silicon bar resonator using internal electrostatic transduction," 13th International Conference on Solid-State Sensors, Actuators and Microsystems (Transducers'05), Seoul, Korea, June 5-9, 2005, pp. 2139-2142.
- [7] R. Candler *et al*, "Single wafer encapsulation of MEMS devices," *IEEE Trans. on Advanced Packaging* **26**(3) pp. 227-232, 2003
- [8] B. Kim, T. Kenny *et al*, "Frequency stability of wafer-scale film encapsulated silicon based MEMS resonators," *Sensors and Actuators A: Physical*, **136**(1) pp. 125-131, 2007
- [9] R. Melamud, *et al*, "Temperature-compensated high-stability silicon resonators," *Applied Physics Letters*, **90** 244107, 2007
- [10] Park, W.T., et al., "Encapsulated submillimeter piezoresistive accelerometers." *Journal of Microelectromechanical Systems*, 15(3): p. 507-514., 2006
- [11] K-L Chen, J. Silvia et al, "Performance Evaluation and Equivalent Model of Silicon Interconnects for Fully-Encapsulated RF MEMS Devices ," *IEEE Trans. on Advanced Packaging*, 2008, *In press*.
- [12] K. Ekinici, M. Roukes *et al*, "Balanced electronic detection of displacement in nanoelectromechanical systems," *Applied Physics Letters* **81** 2253, 2002
- [13] P. Rantakari *et al*, "Reducing the effect of parasitic capacitance on MEMS measurements," *Transducer*, pp. 1556-1559, 2001